

PULMONARY VEIN IMAGING

## A Method for the Determination of Proximal Pulmonary Vein Size Using Contrast-Enhanced Magnetic Resonance Angiography

Thomas H. Hauser,<sup>1,\*</sup> Susan B. Yeon,<sup>1</sup> Seth McClennen,<sup>1</sup>  
George Katsimaglis,<sup>1</sup> Kraig V. Kissinger,<sup>1</sup> Mark E. Josephson,<sup>1</sup>  
Neil M. Rofsky,<sup>1,2</sup> and Warren J. Manning<sup>1,2</sup>

<sup>1</sup>Department of Medicine, Cardiovascular Division,  
Beth Israel Deaconess Medical Center, Boston,  
Massachusetts, USA

<sup>2</sup>Department of Radiology, Harvard Medical School,  
Boston, Massachusetts, USA

### ABSTRACT

*Objectives:* We sought to develop a reproducible method for characterizing the anatomy of the proximal pulmonary veins. *Background:* Contrast-enhanced three-dimensional magnetic resonance angiography (CE-MRA) is a commonly requested test before and after radiofrequency ablation for the treatment of atrial fibrillation. While CE-MRA readily visualizes the pulmonary veins, there is no standardized method for determining their size and cross-sectional anatomy. *Methods:* Data for 24 consecutive patients referred for pulmonary vein CE-MRA before an elective ablation procedure for the treatment of atrial fibrillation were analyzed. Detailed measurements of the pulmonary vein diameter, circumference, and cross-sectional area were obtained at three locations: the juncture of the pulmonary vein with the left atrium (LA) (position 1<sub>J</sub>), the narrowest segment within 5 mm of the juncture (position 2<sub>5mm</sub>), and at the location in the sagittal plane at which the pulmonary veins separate from the LA and from each other (position 3<sub>Sag</sub>). Intraobserver and interobserver variabilities were also determined for each method. *Results:* The left lower pulmonary vein was significantly smaller than the other pulmonary veins at positions 1<sub>J</sub> and 2<sub>5mm</sub> ( $p < 0.05$ ). The right upper pulmonary vein was significantly larger than the other pulmonary vein at position 3<sub>Sag</sub> ( $p < 0.05$ ). At positions 1<sub>J</sub> and 2<sub>5mm</sub>, the diameter had a low correlation with the circumference and cross-sectional

\*Correspondence: Thomas H. Hauser, M.D., Department of Medicine, Cardiovascular Division, Beth Israel Deaconess Medical Center, 330 Brookline Ave., Boston, MA 02215, USA; Fax: (617) 975-5480; E-mail: thauser@bidmc.harvard.edu.

area. At position  $3_{\text{Sag}}$ , the major and minor axis dimensions had a very high correlation with the circumference and cross-sectional area. The intraobserver and interobserver variabilities were substantially lower (better) for position  $3_{\text{Sag}}$ . *Conclusions:* Pulmonary vein diameter measurements are highly variable and do not reflect true anatomic variation in cross-sectional anatomy. A sagittal method of determining pulmonary vein size was highly reproducible and may therefore be advantageous for use in patients likely to need serial examinations.

*Key Words:* Pulmonary vein; Magnetic resonance; Angiography.

## INTRODUCTION

With the advent of radiofrequency ablation of the pulmonary veins (PV) for the prevention of recurrent atrial fibrillation (AF) (Oral et al., 2002; Pappone et al., 2000), there has been renewed interest in assessing PV anatomy to assist in appropriate ablation catheter design, selection, and positioning and to monitor for post-ablation PV stenosis. (Kato et al., 2003; Lin et al., 2000; Moak et al., 2000; Saad et al., 2003; Scanvacca et al., 2000; Wittkamp et al., 2003; Yang et al., 2001) Contrast-enhanced three-dimensional (3D) magnetic resonance angiography (CE-MRA) (Greil et al., 2002; Masui et al., 1991) and computed tomography (Perez-Lugones et al., 2003) readily demonstrate the PV. Although PV diameter is commonly reported (Dill et al., 2003; Kawahira et al., 1997; Lin et al., 2000; Tsao et al., 2001; Wittkamp et al., 2003), there is no standard location or orientation for its measurement, and the variation in diameter measurements has not been determined. In addition, given the asymmetric cross-section of the PV (Wittkamp et al., 2003), the circumference and the cross-sectional area (CSA) may provide more useful anatomic measurements.

To address this issue, we performed detailed measurements of PV diameter, circumference, and CSA in a consecutive series of patients referred for PV CE-MRA.

## METHODS

### Patient Selection

Data from 24 consecutive patients referred for CE-MRA evaluation of PV anatomy before elective AF ablation from October 2001 to September 2002 were included in the study population. Patients with contraindications to CE-MRA were excluded (e.g., pacemaker, intraauricular implants, or intracranial clips). The study was approved by the hospital Committee on Clinical Investigation.

## CE-MRA Protocol

CE-MRA was performed using a 1.5-Tesla whole-body MR system (Gyrosan NT, Philips Medical Systems, Best, The Netherlands) with a five-element cardiac synergy coil for radiofrequency signal reception. First pass breath-hold 3D CE-MRA of the PV was obtained after manual administration of a bolus of 0.2 mmol/kg bolus of gadopentetate dimeglumine (Berlex Laboratories, Wayne, NJ), immediately followed by a saline flush. Data acquisition began after a delay determined by a small timing bolus given before CE-MRA. Breath-holding was performed at end-expiration. Total breath-hold and imaging time was 22 seconds. A spoiled 3D gradient echo sequence with the following parameters was used: repetition time 3.6 ms, echo time 1.1 ms, flip angle 30 degrees, 50 slices, slice thickness 4 mm interpolated to 2 mm, field of view 480 mm, matrix  $272 \times 512$ . Images were prospectively acquired in the axial plane ( $N=19$ ) or coronal plane ( $N=5$ ), and standard, commercially available software on the system was used to generate multiplanar reformations for further evaluation.

## PV Measurement

The PV were measured at three positions (Fig. 1): at the visually apparent juncture of the PV with the left atrium (LA) (Fig. 1B; position  $1_j$ ), at the narrowest segment (smallest diameter) within 5 mm of the juncture (Fig. 1B; position  $2_{5\text{mm}}$ ), and at the location in the sagittal plane at which the PV separate from the LA and from each other (Figs. 1D and E; position  $3_{\text{Sag}}$ ) identified by viewing a sagittal plane reconstruction of the dataset and identifying the position at which the PV separated from the LA and from each other. For positions  $1_j$  and  $2_{5\text{mm}}$ , the maximal diameter at each location was measured in the axial plane for the lower PV and in the coronal plane for the upper PV. The circumference and CSA were measured from an orthogonal reconstruction of the 3D MRA dataset at the same anatomic locations (Figs. 1B and C). For

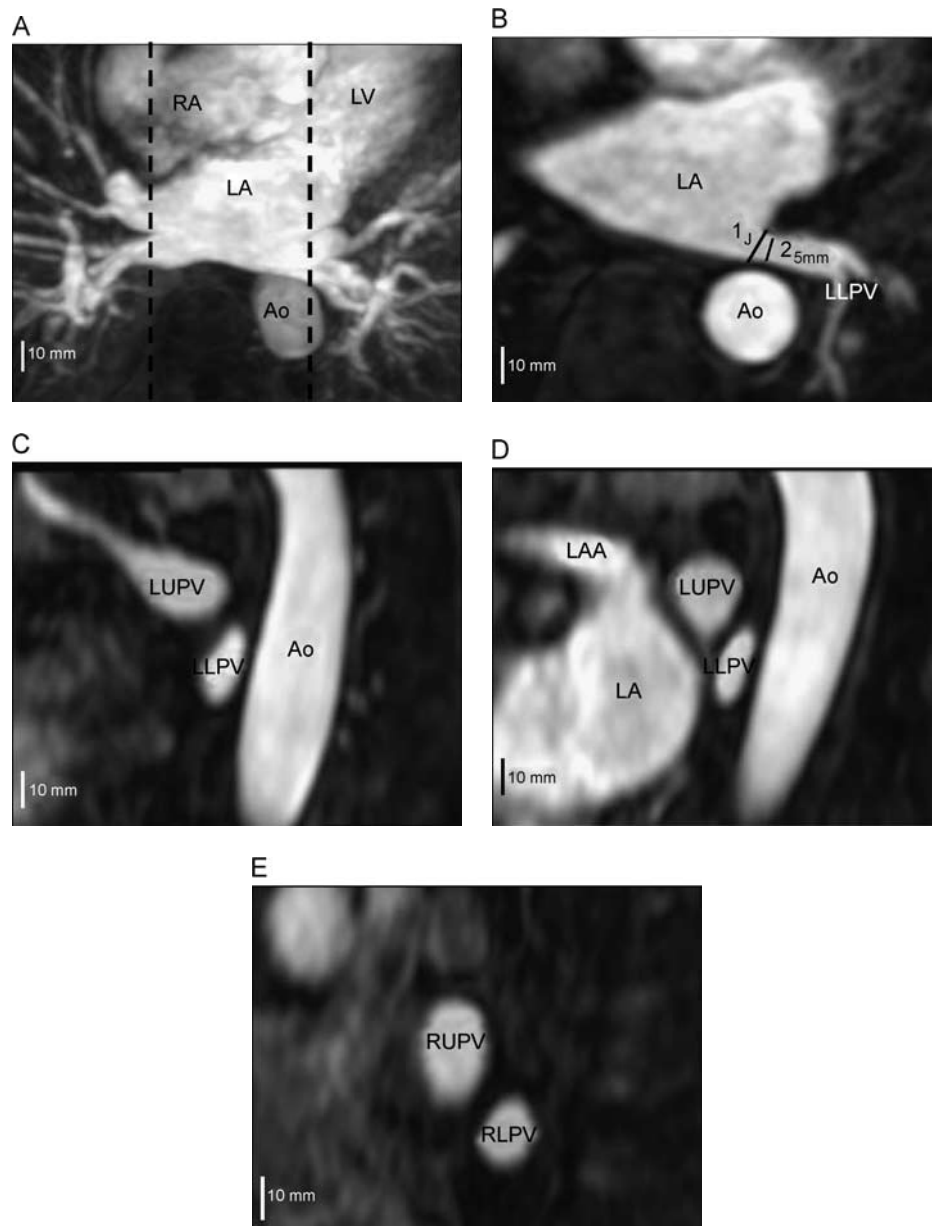


**Figure 1.** Anatomic locations of pulmonary vein (PV) measurement for 3D CE-MRA. (A) 40-mm maximal intensity projection in the axial plane that includes the left atrium (LA), right atrium (RA), left ventricle (LV), and descending aorta (Ao). The dashed lines correspond to the right and left measurement planes for position  $3_{\text{Sag}}$ . (B) 2-mm axial plane through the left lower PV (LLPV) at its maximal diameter. Line  $1_j$  corresponds to the visually apparent juncture of the PV with the LA (position  $1_j$ ). Line  $2_{5\text{mm}}$  corresponds to the narrowest segment within 5 mm of the juncture (position  $2_{5\text{mm}}$ ). (C) LLPV in the plane orthogonal to position  $1_j$  (thickness 2 mm). (D) Left upper PV (LUPV) and the LLPV in the sagittal plane (position  $3_{\text{Sag}}$ ), corresponding to the dashed line in Fig. 1A through the left-sided PV (thickness 2 mm). The left atrial appendage (LAA) is also apparent. (E) Right lower PV (RLPV) and right upper PV (RUPV) in the sagittal plane (position  $3_{\text{Sag}}$ ), corresponding to the dashed line in Fig. 1A through the right-sided PV (thickness 2 mm).

position  $3_{\text{Sag}}$ , the major and minor axes were measured in lieu of the diameter and a circularity index (major axis/minor axis) was calculated. The maximal LA dimension was measured in the axial plane. Two independent observers (T.H.H., G.K.) performed measurements on the entire dataset. Intraobserver error was also assessed by repeat measurements separated by more than 2 weeks.

### Calculation of Predicted Values

To predict the circumference and CSA from the diameter measurements at positions  $1_J$  and  $2_{5\text{mm}}$ , we assumed that the cross-sectional anatomy of the PV was circular. We calculated the predicted circumference as  $\pi \times \text{diameter}$  and the predicted CSA as  $\pi \times (\text{diameter}/2)^2$ . For position  $3_{\text{Sag}}$ , we assumed that the cross-sectional anatomy of the PV was elliptical and calculated the predicted circumference as  $\pi \times ((\text{major axis}/2) + (\text{minor axis}/2))$  and the predicted CSA as  $\pi \times (\text{major axis}/2) \times (\text{minor axis}/2)$ .

### Statistical Analysis

Ordinal variables were presented as counts and percentages. Continuous variables were presented as the mean  $\pm$  standard deviation or as the median and the 95% confidence interval (CI). Measurements performed on different pulmonary veins were compared with an analysis of variance using the Student-Newman-Keuls procedure for multiple comparisons. Ninety-five percent

CI for the index of circularity was calculated by rank order assuming an asymmetric distribution. Observer variations were calculated as the root of the mean squared differences between corresponding observations, divided by the average of the observations. Observer variations were further analyzed with standard linear regression. The correlation between predicted and true measurements was evaluated with standard linear regression and limits of agreement analysis according to the method of Bland and Altman (1986). A two-sided  $p$  value of  $<0.05$  was used to determine statistical significance. Analyses were performed with SAS statistical software (v 8.2, SAS Institute, Cary, NC).

## RESULTS

### Patient Characteristics

Data for 24 consecutive patients with a history of AF were evaluated. Patient demographics are summarized in Table 1. The majority of patients were men. Hypertension and diabetes mellitus were the most common comorbid conditions. The left atrial dimension was mildly increased at  $42 \pm 6$  mm.

### Pulmonary Vein Measurements

Twenty-two patients had two right (upper and lower) and two left (upper and lower) PV that entered the LA. Two patients lacked a distinct left lower

**Table 1.** Characteristics of the study patients.

	Study cohort (N=24)
<i>Demographic characteristics</i>	Mean $\pm$ SD [range]
Male gender [N (%)]	20 (84)
Age (yrs)	56 $\pm$ 10 [39–78]
BSA (m <sup>2</sup> )	2.08 $\pm$ 0.20 [1.58–2.46]
LA dimension (mm)	42 $\pm$ 6 [19–54]
<i>Comorbidities</i>	N (%)
Hypertension	10 (42)
Obstructive sleep apnea	6 (25)
At least moderate mitral regurgitation	5 (21)
Diabetes mellitus	4 (17)
Left ventricular ejection fraction $<40\%$	3 (13)
Coronary artery disease	3 (13)
Constrictive pericarditis	1 (4)
Chronic obstructive lung disease	1 (4)
No comorbidity	5 (21)

Note: BSA—body surface area, LA—left atrium.

**Table 2.** Pulmonary vein size.

Vein	N	Position I <sub>J</sub>			Position 2 <sub>5mm</sub>			Position 3 <sub>Sag</sub>			
		D (mm)	Circ (mm)	CSA (mm <sup>2</sup> )	D (mm)	Circ (mm)	CSA (mm <sup>2</sup> )	Major (mm)	Minor (mm)	Circ (mm)	CSA (mm <sup>2</sup> )
Left lower	22	12.1±2.5*	50±10*	178±69*	10.0±2.3*	45±6*	140±42*	18.1±2.8	11.3±3.4	50±8	167±62
Right lower	24	18.6±3.4	66±13	344±129	15.6±3.0	54±10	235±89	18.8±3.6	12.3±3.1	55±10	213±77
Left upper	24	18.3±3.1	62±11	282±102	15.7±3.1	56±12	228±88	19.8±4.6	15.6±3.2	58±11	253±85
Right upper	24	17.7±2.7	62±11	294±98	16.0±2.5	55±8	229±70	25.2±6.6*	16.8±4.6*	70±16*	352±168*

Note: Circ—circumference, CSA—cross-sectional area, D—diameter, Major—major axis dimension, Minor—minor axis dimension.

\**p*<0.05 vs. other pulmonary veins.

PV, and four patients had a distinct right middle PV. Data for the four major PV were analyzed. Data for diameter, CSA, and circumference measurements obtained for each PV at each of the three measurement positions are summarized in Table 2. At positions 1<sub>J</sub> and 2<sub>5mm</sub>, the left lower PV had a significantly smaller diameter, circumference, and CSA compared with the other PV ( $p < 0.05$ ). At position 3<sub>Sag</sub>, the right upper PV had a significantly larger major axis, circumference, and CSA compared with the other PV ( $p < 0.05$ ).

An index of circularity was also calculated for each PV. The left lower PV was the least circular (median 1.73, 95% CI 1.12 to 2.67) and the left upper

PV was most circular (median 1.28, 95% CI 1.00 to 1.73). Intermediate results were found for the right lower PV (median 1.61, 95% CI 1.07 to 2.50) and right upper PV (median 1.55, 95% CI 1.13 to 2.10).

### Comparison of Predicted and True Measurements

To determine whether diameter measurements reflect the circumference and CSA, we compared the measured values to values predicted by diameter measurements. Linear regression revealed a low correlation between the circumference and CSA as predicted by

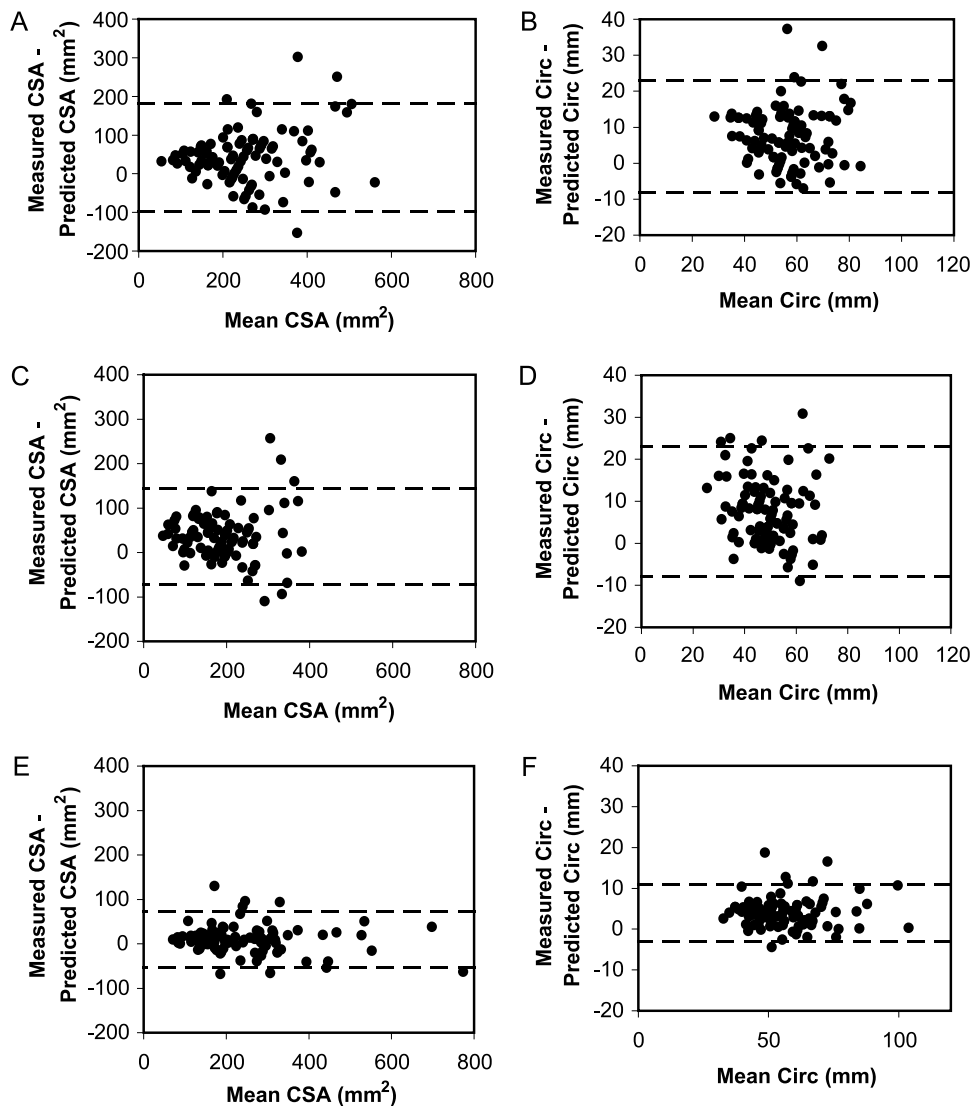


**Figure 2.** Limits of agreement (Bland–Altman) plots comparing the cross-sectional area (CSA) and circumference (Circ) as predicted by the PV diameter to their measured values. (A–B) Comparison for position 1<sub>J</sub>. (C–D) Comparison for position 2<sub>5mm</sub>. (E–F) Comparison for position 3<sub>Sag</sub>. Dashed lines denote the 95% limits of agreement.

**Table 3.** Intraobserver and interobserver variability for pulmonary vein measurement locations.

	Position 1 <sub>J</sub>			Position 2 <sub>5mm</sub>			Position 3 <sub>Sag</sub>			
	D (mm)	Circ (mm)	CSA (mm <sup>2</sup> )	D (mm)	Circ (mm)	CSA (mm <sup>2</sup> )	Major (mm)	Minor (mm)	Circ (mm)	CSA (mm <sup>2</sup> )
<i>Intraobserver</i>										
Variability (%)	13.9	17.3	33.2	12.6	13.2	26.9	8.7	9.1	6.4	12.0
Mean difference ±SD	0.1 ± 2.3	-1 ± 10	-8 ± 93	0.0 ± 1.8	0 ± 7	0 ± 57	0.4 ± 1.8	0.1 ± 1.3	-1 ± 4	-8 ± 28
SEE	2.2	9	82	1.8	7	54	1.7	1.2	3	27
R <sup>2</sup>	0.68	0.45	0.51	0.76	0.57	0.59	0.89	0.91	0.93	0.95
<i>Interobserver</i>										
Variability (%)	23.6	26.6	50.6	23.6	27.5	51.3	12.3	14.0	9.9	17.7
Mean difference ±SD	0.9 ± 3.7	-7 ± 15	-65 ± 143	0.5 ± 3.3	-7 ± 14	-58 ± 109	0.1 ± 2.5	-0.7 ± 1.9	0 ± 6	-4 ± 44
SEE	3.4	11	104	3.0	9	72	2.3	1.6	6	42
R <sup>2</sup>	0.27	0.16	0.20	0.35	0.20	0.26	0.78	0.80	0.83	0.87

Note: SEE—standard error of the estimate.

the diameter and the true measurements for the same PV at position 1<sub>J</sub> ( $R^2=0.62$  and  $0.63$ , respectively) and position 2<sub>5mm</sub> ( $R^2=0.56$  and  $0.61$ , respectively). Similarly, the limits of agreement were wide for both the circumference and CSA comparisons at position 1<sub>J</sub> (23 mm to  $-8$  mm and  $183$  mm<sup>2</sup> to  $-97$  mm<sup>2</sup>, respectively) and position 2<sub>5mm</sub> (23 mm to  $-8$  mm and  $144$  mm<sup>2</sup> to  $-72$  mm<sup>2</sup>, respectively) (Fig. 2A–D). The correlations of the circumference and the CSA as predicted by the major and minor axial dimensions (position 3<sub>Sag</sub>) with the true CSA were very high ( $R^2=0.93$  and  $0.94$ , respectively), and the limits of agreement were narrower (11 mm to  $-3$  mm and  $73$  mm<sup>2</sup> to  $-52$  mm<sup>2</sup>, respectively) (Figs. 2E–F).

### Intraobserver and Interobserver Variability

There was relatively wide intraobserver and interobserver variability for all measures of PV size at positions 1<sub>J</sub> and 2<sub>5mm</sub> (Table 3). For position 3<sub>Sag</sub>, the intraobserver and interobserver variability was much less and the correlation between different measurements was high.

## DISCUSSION

Knowledge of PV anatomy is important for the appropriate planning and follow-up of PV ablation procedures for the treatment of atrial fibrillation. The ability to obtain accurate and reproducible measurements of the PV is desirable and to our knowledge has not been previously investigated. While PV diameter measurements are typically reported in the literature (Dill et al., 2003; Kawahira et al., 1997; Lin et al., 2000; Tsao et al., 2001; Wittkamp et al., 2003), our results suggest that these data may be highly variable. Furthermore, diameter measurements do not reflect the variation in circumference or CSA, likely due to the asymmetric geometry of the pulmonary veins, most prominently of the left lower PV. We believe the circumference and CSA are more logical assessments and appear to yield more reliable anatomic measurements. Measurement values obtained using the sagittal method (position 3<sub>Sag</sub>) were highly reproducible and may therefore be advantageous for patients requiring serial evaluation.

### PV Measurements

We chose three positions for PV measurement. Diameter measurements at position 1<sub>J</sub> or in the proximal

PV near position 2<sub>5mm</sub> are the most commonly reported measures of PV size for x-ray angiography, CE-MRA, and CTA (Dill et al., 2003; Kawahira et al., 1997; Lin et al., 2000; Tsao et al., 2001; Wittkamp et al., 2003). Position 3<sub>Sag</sub> was selected because of its ease in evaluating the juncture of the PV with the LA and because the major axis, minor axis, circumference and CSA can all be measured in a single, predefined imaging plane.

Three-dimensional MRA datasets offer the advantage of image reconstruction in any desired plane. Although PV diameter is frequently used as a single measure of PV size, the circumference or CSA may be more appropriate in the determination of catheter size or stenosis, respectively. We therefore measured the circumference and CSA in the plane orthogonal to the diameter at positions 1<sub>J</sub> and 2<sub>5mm</sub>. For both positions, the diameter did not accurately predict the circumference or the CSA, likely due to the asymmetric cross-sectional anatomy of the PV. There does not appear to be a simple relationship between diameter measurements and PV cross-sectional anatomy. Measurements of the major and minor axial dimensions at position 3<sub>Sag</sub>, assuming an elliptical PV cross-sectional anatomy, more accurately predicted the circumference and CSA.

### Intraobserver and Interobserver Variability

The intraobserver and interobserver variability were high for all measures of PV size at positions 1<sub>J</sub> and 2<sub>5mm</sub>. Identifying the juncture of a PV with the LA is a highly subjective process as there is a smooth transition between the two structures. It was thus difficult to ensure a consistent measurement location for both the diameter and, in the reconstructed orthogonal plane, the circumference and CSA, reflected in the high variability between different observations. Positions 1<sub>J</sub> and 2<sub>5mm</sub> may therefore be less desirable for serial assessment. The sagittal imaging plane for position 3<sub>Sag</sub> was consistent for each patient and the separation of the PV from the LA and from each other is distinct. This method for identifying the proximal PV allowed for consistent measurement location and a correspondingly low variability and high correlation between different observations.

### Limitations

All patients in the study had a history of atrial fibrillation; this may comprise a unique population, potentially limiting the ability to apply these data to non-atrial fibrillation populations. We did not assess the accuracy of PV measurements in comparison to

direct anatomic findings at autopsy or with x-ray data. We determined the intraobserver and interobserver variability by repeating measurements on the same dataset; the variability for serial studies in the same patient is unknown. Changes in hemodynamic parameters such as cardiac output and LA pressure before and after PV ablation may increase the variability between observations without a true change in PV size. Although position  $3_{\text{sag}}$  is located within the proximal PV, it may not coincide with the location of catheter ablation or clinically important PV stenosis. The method described for the determination of PV size was developed using 3D imaging and may not be applicable to tomographic or projection imaging.

### Conclusions

PV diameter measurements alone do not reflect true anatomic variation and are highly variable between different observations. CE-MRA using the sagittal method of determining PV size was highly reproducible for all measures and may therefore be advantageous for patients likely to need serial examinations.

### ACKNOWLEDGMENTS

Dr. Hauser is supported in part by the Clinical Investigator Training Program, Beth Israel Deaconess Medical Center-Harvard/MIT Health Sciences and Technology, in collaboration with Pfizer Inc.

### REFERENCES

- Bland, J. M., Altman, D. G. (1986). Statistical methods for assessing agreement between two methods of measurement. *Lancet* 1:307–310.
- Dill, T., Neumann, T., Ekin, O., Breidenbach, C., John, A., Erdogan, A., Bachmann, G., Hamm, C. W., Pitschner, H.-F. (2003). Pulmonary vein diameter reduction after radiofrequency catheter ablation for paroxysmal atrial fibrillation evaluated by contrast-enhanced three-dimensional magnetic resonance imaging. *Circulation* 107(6): 845–850.
- Greil, G., Powell, A., Gildein, H., Geva, T. (2002). Gadolinium-enhanced three-dimensional magnetic resonance angiography of pulmonary and systemic venous anomalies. *J. Am. Coll. Cardiol.* 39(2): 335–341.
- Kato, R., Lickfett, L., Meininger, G., Dickfeld, T., Wu, R., Juang, G., Angkeow, P., Lacorte, J., Bluemke, D., Berger, R., Halperin, H. R., Calkins, H. (2003). Pulmonary vein anatomy in patients undergoing catheter ablation of atrial fibrillation: lessons learned by use of magnetic resonance imaging. *Circulation* 107(15):2004–2010.
- Kawahira, Y., Kishimoto, H., Kawata, H., Ikawa, S., Euda, H., Nakajima, T., Kayatani, F., Inamura, N., Nakada, T. (1997). Diameters of the pulmonary arteries and veins as an indicator of bilateral and unilateral pulmonary blood flow in patients with congenital heart disease. *J. Card. Surg.* 12(4): 253–260.
- Lin, W. S., Prakash, V. S., Tai, C. T., Hsieh, M. H., Tsai, C. F., Yu, W. C., Lin, Y. K., Ding, Y. A., Chang, M. S., Chen, S. A. (2000). Pulmonary vein morphology in patients with paroxysmal atrial fibrillation initiated by ectopic beats originating from the pulmonary veins: implications for catheter ablation. *Circulation* 101(11):1274–1281.
- Masui, T., Seelos, K. C., Kersting-Sommerhoff, B. A., Higgins, C. B. (1991). Abnormalities of the pulmonary veins: evaluation with MR imaging and comparison with cardiac angiography and echocardiography. *Radiology* 181:645–649.
- Moak, J., Moore, H., Lee, S., Giglia, T., Sable, C., Furbush, N., Ringel, R. (2000). Case report: pulmonary vein stenosis following RF ablation of paroxysmal atrial fibrillation. Successful treatment with balloon dilation. *J. Interv. Cardiol. Electrophysiol.* 4:621–631.
- Oral, H., Knight, B. P., Tada, H., Ozaydin, M., Chugh, A., Hassan, S., Scharf, C., Lai, S. W., Greenstein, R., Pelosi, F., Jr., Strickberger, S. A., Morady, F. (2002). Pulmonary vein isolation for paroxysmal and persistent atrial fibrillation. *Circulation* 105: 1077–1081.
- Pappone, C., Rosanio, S., Oreto, G., Tocchi, M., Gugliotta, F., Vicedomini, G., Salvati, A., Dicandia, C., Mazzone, P., Santinelli, V., Gulletta, S., Chierchia, S. (2000). Circumferential radiofrequency ablation of pulmonary vein ostia. A new anatomic approach for curing atrial fibrillation. *Circulation* 102:2619–2628.
- Perez-Lugones, A., Schwartzman, P. R., Schweikert, R., Tchou, P. J., Saliba, W., Marrouche, N. F., Castle, L. W., White, R. D., Natale, A. (2003). Three-dimensional reconstruction of pulmonary veins in patients with atrial fibrillation and controls: morphological characteristics of different veins. *Pacing Clin. Electrophysiol.* 26(1 Pt 1):8–15.
- Saad, E. B., Marrouche, N. F., Saad, C. P., Ha, E., Bash, D., White, R. D., Rhodes, J., Prieto, L., Martin, D.

- O., Saliba, W. I., Schweikert, R. A., Natale, A. (2003). Pulmonary vein stenosis after catheter ablation of atrial fibrillation: emergence of a new clinical syndrome. *Ann. Intern. Med.* 138:634–638.
- Scanavacca, M., Kajita, L., Vieira, M., Sosa, E. (2000). Pulmonary vein stenosis complicating catheter ablation of focal atrial fibrillation. *J. Cardiovasc. Electrophysiol.* 1:677–681.
- Tsao, H., Yu, W., Cheng, H., Wu, M., Tai, C., Lin, W., Ding, Y., Chang, M., Chen, S. (2001). Pulmonary vein dilation in patients with atrial fibrillation: detection by magnetic resonance imaging. *J. Cardiovasc. Electrophysiol.* 12:809–813.
- Wittkamp, F. H., Vonken, E. J., Derksen, R., Loh, P., Velthuis, B., Wever, E. F., Boersma, L. V., Rensing, B. J., Cramer, M. J. (2003). Pulmonary vein ostium geometry: analysis by magnetic resonance angiography. *Circulation* 107:21–23.
- Yang, M., Akbari, H., Reddy, G. P., Higgins, C. B. (2001). Identification of pulmonary vein stenosis after radiofrequency ablation for atrial fibrillation using MRI. *J. Comput. Assist. Tomogr.* 25: 34–35.

Submitted December 10, 2003

Accepted April 7, 2004